JAERI-M
89-116

NUMERICAL INVESTIGATION OF CURRENT PROFILE FLATTENING DURING LOWER HYBRID CURRENT DRIVE IN JT-60

September 1989

Ryuji YOSHINO, Kenkichi USHIGUSA, Tsuyoshi IMAI
Hiroshi SHIRAI and Katsuhiro SHIMIZU

日本原子力研究所
Japan Atomic Energy Research Institute

JAERI-M レポートは，日本原子力研究所が不定期に公刊している研究報告書です。
入手の問合わせは，日本原子力研究所技術情報部情報資料課（〒319−11 茨城県那珂郡東海村）あて，お申しこしください。なお，このほかに財団法人原子力弘済会資料センター（〒319-11 茨城県那珂郡東海村日本原子力研究所内）で複写による実費領布をおこなっております。

JAERI-M reports are issued irregularly.
Inquiries about availability of the reports should be addressed to Information Division, Department of Technical Information, Japan Atomic Energy Research Institute, Tokai-mura, Naka-gun, Ibaraki-ken 319-11, Japan.

編集兼発行　日本原子力研究所
印　　刷　山田軽印刷所

JAERI-M 89-116

Numerical Investigation of Current Profile Flattening during Lower Hybrid Current Drive in JT-60

Ryuji YOSHINO, Kenkichi USHIGUSA, Tsuyoshi IMAI, Hiroshi SHIRAI and Katsuhiro SHIMIZU

Department of Large Tokamak Research
Naka Fusion Research Establishment
Japan Atomic Energy Research Institute
Naka-machi, Naka-gun, Ibaraki-ken

(Received August 4, 1989)

The mechanism that makes the broader current profile during LHCD has been numerically investigated in the case of JT-60. A one path absorption model of LHW with a bi-maxwellian electron distribution can explain well the experimental observation of the current profile flattening. Furthermore the MHD instability calculated from the simulated current profile is consistent with the measured MHD activity.

Keywords: JT-60, Lower Hybrid Current Drive, Current Profile, MHD Activities

JAERI－M 89－116

JT－60 LHCDによる電流分布平担化のシミュレーション解析

日本原子力研究所那珂研究所臨界プラズマ研究部
芳野　隆治・牛草　健吉・今井　　剛
白井　　浩・清水　勝宏

（1989年8月4日受理）

JT－60 LHCD実験にて得られる電流分布の平担化の機構について，計算機シミュレーション解析を行なった。一回の波動伝搬により，低減混成波が二成分のマクスウェル分布をもつ電子に吸収されるとするモデルが電流分布の平担化の実験結果をよく説明できる。さらに，シミュレーションにて得られた電流分布より評価されるMHD挙動は，測定されたMHD挙動とよく一致している。

那珂研究所：〒311-01　茨城県那珂郡那珂町大字向山801－1

Contents

目　　次

1. Introduction

Control of the current profile is one of the key issues to improve the confinement of energy. Modification of the current profile by LHCD was performed in ASDEX, and the stabilization of sawteeth was achieved increasing q(0) above 1 with 30% improvement in energy confinement at q(a)=3.6[1]. Neutral Beam (NB) heating of noninductively current driven plasma by LHRF was also conducted in JT-60 large Tokamak, where the broader current profile modified by LHCD just before NB heating clearly improved the energy confinement and the confinement time for the incremental stored energy was raised by 20-30%[2].

These experimental results suggest that a broader current profile is useful to improve the energy confinement and that LHCD is one of the promising method to flatten the current profile. In order to explain the experimental results of LHCD experiments, the upshift in the $N_{//}$ spectrum of launched LHW is assumed, without that LHW cannot drive current. Some theoretical models have been proposed in order to explain the mechanism of the upshift such as the multiple-reflection[3],[4], the random phase approximation[5], or the scattering owing to magnetic ripple[6], but have not been clarified yet experimentally.

Here, we would like to show that a one path absorption model assuming the presence of high energy electrons produced by LHW, that fulfills the spectrum gap, can explain well the modification of the current profile in the LHCD experiment on JT-60. The current profile noninductively driven by LHRF is calculated using the Brambilla theory [7] for the $N_{//}$ spectrum of LHW, a ray tracing code[8], and a one-dimensional Fokker-Planck equation[9] for the power deposition of LHW to RF current. The anomalous diffusion of the RF current[4] is not included, because that has not been clarified experimentally yet. The modification of the current profile after the onset of LHCD has been investigated by the diffusion equation of the poloidal magnetic field. Then the time evolution of plasma internal inductance (l_i) and the loop voltage (V_l), that is experimentally obtained, has been reproduced by adjusting the ratio of the density and temperature of the high energy electron tail to the bulk

electron. Furthermore MHD stability analysis of the simulated current profile has been compared with MHD activities measured by soft X-ray detectors.

2. Experimental Results

The typical experimental result of LHCD in JT-60 is presented in Fig.1(a) with solid lines, where LHRF of 2GHz with $\Delta\phi=90(N_{//}=1.7,\ \Delta N_{//}=1.0)$ is injected for about 2sec to the ohmic diverted plasma of 1MA with $\bar{n}_e=0.3X10^{19}/m^3$ and $q_{eff}=5.7(Bt=4T)$.

The loop voltage drops after the onset of LHCD. On the other hand, the Shafranov Lambda($=\beta p+li/2$) obtained by magnetics rises a little by 0.04; after which it decreases slowly with the rate of -0.06/sec. At about 200msec after the onset of LHCD, the loop voltage becomes slightly negative, implying the plasma current is fully driven by LHCD. Then $\beta p+li/2$ drops from 0.93 to 0.78 over about 2sec. The internal inductance l_i, obtained from the Faraday rotation measurement along one vertical chord located at half minor radius, suggests that the decrease in $\beta p+li/2$ is caused by the drop in li[10]. The increase in βp due to the superthermal electrons is estimated to be 0.02-0.06, assuming all of the noninductive current is carried by superthermal quasilinear plateau electrons extending to the accessibility limit. Therefore the decrease in l_i is about -0.3. Sawteeth activities disappears a little after the onset of LHCD.

3. Simulation Model

The current profile driven by LHW is calculated by the following three codes. The power spectrum launched from the antenna is calculated by the Brambilla code. The power spectrum is divided into 200 rays. The propagation of each ray is calculated following the ray equations of $dr/dt=\delta\Omega/\delta k, dk/dt=\delta\Omega/\delta r$, where $\Omega(k,r,t)=0$ is the dispersion relation of the cold plasma approximation. This ray tracing code is the single path code and the large upshift of $N_{//}$ due to the multiple reflection is not contained. Hence a large spectrum gap exists between the velocity of the thermal electrons and the phase velocity of LHW radiated from launcher. In order to remove this spectrum gap an assumption of the high energy electron tail produced by LHW is employed here without considering the production mechanism of that. The distribution function of that can be presented as the solution of the one-dimensional Fokker-Planck equation as follows.

electron. Furthermore MHD stability analysis of the simulated current profile has been compared with MHD activities measured by soft X-ray detectors.

2. Experimental Results

The typical experimental result of LHCD in JT-60 is presented in Fig.1(a) with solid lines, where LHRF of 2GHz with $\Delta\phi=90(N_{//}=1.7,\ \Delta N_{//}=1.0)$ is injected for about 2sec to the ohmic diverted plasma of 1MA with $\bar{n}_e=0.3X10^{19}/m^3$ and $q_{eff}=5.7(Bt=4T)$.

The loop voltage drops after the onset of LHCD. On the other hand, the Shafranov Lambda($=\beta p+li/2$) obtained by magnetics rises a little by 0.04; after which it decreases slowly with the rate of -0.06/sec. At about 200msec after the onset of LHCD, the loop voltage becomes slightly negative, implying the plasma current is fully driven by LHCD. Then $\beta p+li/2$ drops from 0.93 to 0.78 over about 2sec. The internal inductance l_i, obtained from the Faraday rotation measurement along one vertical chord located at half minor radius, suggests that the decrease in $\beta p+li/2$ is caused by the drop in li[10]. The increase in βp due to the superthermal electrons is estimated to be 0.02-0.06, assuming all of the noninductive current is carried by superthermal quasilinear plateau electrons extending to the accessibility limit. Therefore the decrease in l_i is about -0.3. Sawteeth activities disappears a little after the onset of LHCD.

3. Simulation Model

The current profile driven by LHW is calculated by the following three codes. The power spectrum launched from the antenna is calculated by the Brambilla code. The power spectrum is divided into 200 rays. The propagation of each ray is calculated following the ray equations of $dr/dt=\delta\Omega/\delta k, dk/dt=\delta\Omega/\delta r$, where $\Omega(k,r,t)=0$ is the dispersion relation of the cold plasma approximation. This ray tracing code is the single path code and the large upshift of $N_{//}$ due to the multiple reflection is not contained. Hence a large spectrum gap exists between the velocity of the thermal electrons and the phase velocity of LHW radiated from launcher. In order to remove this spectrum gap an assumption of the high energy electron tail produced by LHW is employed here without considering the production mechanism of that. The distribution function of that can be presented as the solution of the one-dimensional Fokker-Planck equation as follows.

electron. Furthermore MHD stability analysis of the simulated current profile has been compared with MHD activities measured by soft X-ray detectors.

2. Experimental Results

The typical experimental result of LHCD in JT-60 is presented in Fig.1(a) with solid lines, where LHRF of 2GHz with $\Delta\phi=90(N_{//}=1.7,\ \Delta N_{//}=1.0)$ is injected for about 2sec to the ohmic diverted plasma of 1MA with $\bar{n}_e=0.3X10^{19}/m^3$ and $q_{eff}=5.7(Bt=4T)$.

The loop voltage drops after the onset of LHCD. On the other hand, the Shafranov Lambda($=\beta p+li/2$) obtained by magnetics rises a little by 0.04; after which it decreases slowly with the rate of -0.06/sec. At about 200msec after the onset of LHCD, the loop voltage becomes slightly negative, implying the plasma current is fully driven by LHCD. Then $\beta p+li/2$ drops from 0.93 to 0.78 over about 2sec. The internal inductance l_i, obtained from the Faraday rotation measurement along one vertical chord located at half minor radius, suggests that the decrease in $\beta p+li/2$ is caused by the drop in li[10]. The increase in βp due to the superthermal electrons is estimated to be 0.02-0.06, assuming all of the noninductive current is carried by superthermal quasilinear plateau electrons extending to the accessibility limit. Therefore the decrease in l_i is about -0.3. Sawteeth activities disappears a little after the onset of LHCD.

3. Simulation Model

The current profile driven by LHW is calculated by the following three codes. The power spectrum launched from the antenna is calculated by the Brambilla code. The power spectrum is divided into 200 rays. The propagation of each ray is calculated following the ray equations of $dr/dt=\delta\Omega/\delta k, dk/dt=\delta\Omega/\delta r$, where $\Omega(k,r,t)=0$ is the dispersion relation of the cold plasma approximation. This ray tracing code is the single path code and the large upshift of $N_{//}$ due to the multiple reflection is not contained. Hence a large spectrum gap exists between the velocity of the thermal electrons and the phase velocity of LHW radiated from launcher. In order to remove this spectrum gap an assumption of the high energy electron tail produced by LHW is employed here without considering the production mechanism of that. The distribution function of that can be presented as the solution of the one-dimensional Fokker-Planck equation as follows.

$$f_e^{tail}(v_{//})=f_{e0}^{tail}\exp\left[-2\int_0^{v_{//}}\frac{v_{//}/v_{tail}^2}{1+D/C}dv_{//}\right] \quad (1)$$

where D,C are the diffusion coefficients due to LHW and collision, then LH driven current is given as follows.

$$j(r)=\int_{-\infty}^{\infty}-n_e^{tail}(r)ev_{//}f_e^{tail}(v_{//})dv_{//} \quad (2)$$

The diffusion equation of the poloidal magnetic field is used to calculate the time evolution of the current profile during the LHCD. The following assumptions are adopted; 1)Noninductive current is driven just after the onset of LHRF. 2)Total of the noninductive current is almost same with that of plasma current controlled to be constant without the time delay. 3)Resistivity of the noninductive current produced by superthermal electrons is zero. 4)Spitzer resistivity is adopted as that of the inductive current, because in JT-60 the resistivity is the level of Spitzer one and is not the level of the neoclassical one[11].

Then the diffusion equation of the poloidal magnetic field becomes,

$$\dot{B}_p=\frac{d}{dr}\frac{\eta}{\mu_0}\frac{d}{dr}rB_p-\frac{d}{dr}\eta j_{CD} \quad (3)$$

where η is Spitzer resistivity and j_{cd} is the noninductive current driven by LHRF. Then plasma current profile j(r) can be calculated from Bp, then internal inductance (l_i) and the loop voltage (V_l) can be obtained.

The electron density profile is parabolic with $\bar{n}e=0.3\times10^{19}/m^3$. The profile of electron temperature is assumed as follows, and is kept constant during LHCD.

$$T_e(r)=(T_0-T_{edge})\left[1-(\frac{r}{a})^2\right]^{\alpha}+T_{edge} \quad (4)$$

where Te(o)=3KeV, T_{edge}=300eV, α=5.0 and Zeff=2.0 are adopted to fit the one turn voltage and $\beta_p+l_i/2$ just before the onset of LHCD. The temperature

profile may become more peaked during LHCD owing to the suppression of the sawtooth as measure in ASDEX[12], however that cannot explain the experimentally obtained large decrease in l_i of -0.3 .

MHD stability is analyzed by the usual Δ' method[13]. The time evolution of the magnetic island width of m/n=2/1, 3/2, and 3/1 mode is calculated for the largely modified current profile obtained in the above simulation.

4. Simulation Results

Figure 2(a) presents the contours of the total RF current in the parameter plane of the high energy electron, where n_e(tail)/n_e(bulk) is the ratio of the tail electron density and the bulk electron density and Te(tail)/Te(bulk) is the temperature ratio of the tail electron to the bulk electron. We have adopted tail parameters as denoted in A, B, C, D and E, and the correlated RF current profiles are presented in Fig.2(b). The time evolution of l_i and $\beta p+l_i/2$ are shown in Fig.3, where the difference of the RF current profile leads to different time evolutions. Then we can select the tail parameters that can fit the time evolutions of l_i and $\beta p+l_i/2$ to the experimentally observed ones. The best fit results are presented in Fig.1(a) with ne(tail)/ne(bulk)=0.078 and Te(tail)/Te(bulk)=33. Simulated Vl and βp+li/2 denoted as dashed lines agree well with the experimental data except the phase at the onset of LHCD. The difference during this phase comes from the difference in the injected power, where RF power injected in the experiment is smaller than that employed in the simulation.

The simulated li and q(0) are presented in Fig.1(b) and(c), and profiles of current and safety factor are presented as a function of time in Fig.4(a) and (b). The current density decreases near the plasma center and at the plasma periphery, while it increases near the half radius. The drop in the current density at the plasma periphery is faster than that at the plasma center because of the higher resistivity, that can explain the increase in li just after the onset of LHCD. The decrease in li with long time constant also can be explained by the low resistivity at the plasma center. The center q(0) increases gradually and exceed unity at almost 0.5sec after the onset of LHCD, that well agrees with the experimentally observed time of the disappearance in sawteeth.

profile may become more peaked during LHCD owing to the suppression of the sawtooth as measure in ASDEX[12], however that cannot explain the experimentally obtained large decrease in l_i of -0.3 .

MHD stability is analyzed by the usual Δ' method[13]. The time evolution of the magnetic island width of m/n=2/1, 3/2, and 3/1 mode is calculated for the largely modified current profile obtained in the above simulation.

4. Simulation Results

Figure 2(a) presents the contours of the total RF current in the parameter plane of the high energy electron, where n_e(tail)/n_e(bulk) is the ratio of the tail electron density and the bulk electron density and Te(tail)/Te(bulk) is the temperature ratio of the tail electron to the bulk electron. We have adopted tail parameters as denoted in A, B, C, D and E, and the correlated RF current profiles are presented in Fig.2(b). The time evolution of l_i and $\beta p+l_i/2$ are shown in Fig.3, where the difference of the RF current profile leads to different time evolutions. Then we can select the tail parameters that can fit the time evolutions of l_i and $\beta p+l_i/2$ to the experimentally observed ones. The best fit results are presented in Fig.1(a) with ne(tail)/ne(bulk)=0.078 and Te(tail)/Te(bulk)=33. Simulated Vl and βp+li/2 denoted as dashed lines agree well with the experimental data except the phase at the onset of LHCD. The difference during this phase comes from the difference in the injected power, where RF power injected in the experiment is smaller than that employed in the simulation.

The simulated li and q(0) are presented in Fig.1(b) and(c), and profiles of current and safety factor are presented as a function of time in Fig.4(a) and (b). The current density decreases near the plasma center and at the plasma periphery, while it increases near the half radius. The drop in the current density at the plasma periphery is faster than that at the plasma center because of the higher resistivity, that can explain the increase in li just after the onset of LHCD. The decrease in li with long time constant also can be explained by the low resistivity at the plasma center. The center q(0) increases gradually and exceed unity at almost 0.5sec after the onset of LHCD, that well agrees with the experimentally observed time of the disappearance in sawteeth.

5. MHD Activities

The time evolutions of the location and the width of magnetic island calculated from the simulated current profile are presented in Fig.1(d), where an m=2 island grows gradually near the half radius and an m=3 island appears at about 1.5sec after the onset of LHCD. The change in the position and island width of m=2 mode is small in spite of the large decease in l_i of -0.25.

On the other hand detailed structure of MHD activity at t=5.9sec measured by a soft X-ray detector array is presented in Fig.4(c). The fluctuation near the plasma center is identified to be m=1 oscillation, that can be explained by the toroidal coupling with m=2 mode.

Relatively large fluctuation of 10% with even mode is also observed near the half radius, that can correspond to the simulated m=2 oscillation at q=2 surface. The chord integrated soft X-ray signal is calculated from the simulated island location and width assuming the flattened electron temperature inside the island, and is compared with the observed soft X-ray emission. Solid and broken lines in Fig.5 show the profile at the top and bottom in the fluctuation. Simulated signal fairly agrees with experimentally observed signal, that suggests the location and the width of the m=2 island are well fitted.

Furthermore odd mode is observed at near the plasma periphery (r/a= 0.8), on the other hand m=3 mode is simulated at the same radius. The fluctuation observed at r/a=0.8 may be m=3 mode. Therefore the simulated current profile is consistent to the experimentally observed MHD activities. The flattening of the current profile by LHCD increases the gradient of current density at q=2 and q=3 surface and enhances MHD activities.

6. Conclusions

Investigation in the modification of the current profile during LHCD has been performed. Experimentally obtained time evolution of plasma internal inductance (l_i) and loop voltage (V_l) has been well reproduced by the numerical simulation using a one path absorption model of LHW with a bi-maxwellian electron distribution. Furthermore the MHD stability analysis of the simulated current profile is consistent with the experimentally observed MHD activities.

5. MHD Activities

The time evolutions of the location and the width of magnetic island calculated from the simulated current profile are presented in Fig.1(d), where an m=2 island grows gradually near the half radius and an m=3 island appears at about 1.5sec after the onset of LHCD. The change in the position and island width of m=2 mode is small in spite of the large decease in l_i of -0.25.

On the other hand detailed structure of MHD activity at t=5.9sec measured by a soft X-ray detector array is presented in Fig.4(c). The fluctuation near the plasma center is identified to be m=1 oscillation, that can be explained by the toroidal coupling with m=2 mode.

Relatively large fluctuation of 10% with even mode is also observed near the half radius, that can correspond to the simulated m=2 oscillation at q=2 surface. The chord integrated soft X-ray signal is calculated from the simulated island location and width assuming the flattened electron temperature inside the island, and is compared with the observed soft X-ray emission. Solid and broken lines in Fig.5 show the profile at the top and bottom in the fluctuation. Simulated signal fairly agrees with experimentally observed signal, that suggests the location and the width of the m=2 island are well fitted.

Furthermore odd mode is observed at near the plasma periphery (r/a= 0.8), on the other hand m=3 mode is simulated at the same radius. The fluctuation observed at r/a=0.8 may be m=3 mode. Therefore the simulated current profile is consistent to the experimentally observed MHD activities. The flattening of the current profile by LHCD increases the gradient of current density at q=2 and q=3 surface and enhances MHD activities.

6. Conclusions

Investigation in the modification of the current profile during LHCD has been performed. Experimentally obtained time evolution of plasma internal inductance (l_i) and loop voltage (V_l) has been well reproduced by the numerical simulation using a one path absorption model of LHW with a bi-maxwellian electron distribution. Furthermore the MHD stability analysis of the simulated current profile is consistent with the experimentally observed MHD activities.

Much more flattening of the current profile can be expected by LHW with higher $N_{//}$ spectrum and narrower $\Delta N_{//}$. For this purpose one of the three LHRF launchers of JT-60 has been remodelled to the multi-junction type, and experiments to investigate the controllability of the current profile with this new launcher are now under way.

Acknowledgement

The author would like to acknowledge Drs. Y.Shimomura, M.Azumi for the fruitful discussions and the continuous encouragement. They also wish to express their gratitude to Drs. M.Yoshikawa and S.Tamura for continued encouragement and support.

References

[1] SÖLDNER,F.X., McCormick,K., ECKHARTT,D., et al., J. Phys. Rev. Lett. 57(1986)1137.

[2] JT-60 TEAM presented by IMAI,T., in Plasma Physics and Controlled Nuclear Fusion Research 1986(Proc. 11th Int. Conf. Kyoto, 1986), Vol.1, IAEA, Vienna(1987)563.

[3] BONOLI, P.T., Phys. Fluids 29(1986)2937.

[4] BONOLI, P.T., PORKOLAB, M., TAKASE, T., KNOWLTON, S.F., Nucl. Fusion 28(1988)991.

[5] MOREAU,D., RAX,J.M., and SAMAIN,A., 15th European Conf. on Controlled and Plasma Heating, Dubrovnik, vol.3, (1988) 995.

[6] WEGROWE,J.G., 14th European Conf. on Controlled Fusion and Plasma Physics, Madrid, vol.3, (1987) 911.

[7] BRAMBILLA, M., Nucl. Fusion 16(1976)47.

Much more flattening of the current profile can be expected by LHW with higher $N_{//}$ spectrum and narrower $\Delta N_{//}$. For this purpose one of the three LHRF launchers of JT-60 has been remodelled to the multi-junction type, and experiments to investigate the controllability of the current profile with this new launcher are now under way.

Acknowledgement

The author would like to acknowledge Drs. Y.Shimomura, M.Azumi for the fruitful discussions and the continuous encouragement. They also wish to express their gratitude to Drs. M.Yoshikawa and S.Tamura for continued encouragement and support.

References

[1] SÖLDNER,F.X., McCormick,K., ECKHARTT,D., et al., J. Phys. Rev. Lett. 57(1986)1137.

[2] JT-60 TEAM presented by IMAI,T., in Plasma Physics and Controlled Nuclear Fusion Research 1986(Proc. 11th Int. Conf. Kyoto, 1986), Vol.1, IAEA, Vienna(1987)563.

[3] BONOLI, P.T., Phys. Fluids 29(1986)2937.

[4] BONOLI, P.T., PORKOLAB, M., TAKASE, T., KNOWLTON, S.F., Nucl. Fusion 28(1988)991.

[5] MOREAU,D., RAX,J.M., and SAMAIN,A., 15th European Conf. on Controlled and Plasma Heating, Dubrovnik, vol.3, (1988) 995.

[6] WEGROWE,J.G., 14th European Conf. on Controlled Fusion and Plasma Physics, Madrid, vol.3, (1987) 911.

[7] BRAMBILLA, M., Nucl. Fusion 16(1976)47.

Much more flattening of the current profile can be expected by LHW with higher $N_{//}$ spectrum and narrower $\Delta N_{//}$. For this purpose one of the three LHRF launchers of JT-60 has been remodelled to the multi-junction type, and experiments to investigate the controllability of the current profile with this new launcher are now under way.

Acknowledgement

The author would like to acknowledge Drs. Y.Shimomura, M.Azumi for the fruitful discussions and the continuous encouragement. They also wish to express their gratitude to Drs. M.Yoshikawa and S.Tamura for continued encouragement and support.

References

[1] SÖLDNER,F.X., McCormick,K., ECKHARTT,D., et al., J. Phys. Rev. Lett. 57(1986)1137.

[2] JT-60 TEAM presented by IMAI,T., in Plasma Physics and Controlled Nuclear Fusion Research 1986(Proc. 11th Int. Conf. Kyoto, 1986), Vol.1, IAEA, Vienna(1987)563.

[3] BONOLI, P.T., Phys. Fluids 29(1986)2937.

[4] BONOLI, P.T., PORKOLAB, M., TAKASE, T., KNOWLTON, S.F., Nucl. Fusion 28(1988)991.

[5] MOREAU,D., RAX,J.M., and SAMAIN,A., 15th European Conf. on Controlled and Plasma Heating, Dubrovnik, vol.3, (1988) 995.

[6] WEGROWE,J.G., 14th European Conf. on Controlled Fusion and Plasma Physics, Madrid, vol.3, (1987) 911.

[7] BRAMBILLA, M., Nucl. Fusion 16(1976)47.

[8] BERNSTEIN, I., B., Phys. Fluids 18(1975)320.

[9] FISCH, N., J. Phys. Rev. Lett. 41(1978)873.

[10] JT-60 TEAM presented by YOSHINO, R., Plasma Physics and Controlled Fusion 29(1987)1377.
and FUKUDA.T., et al., to be published to Nuclear Fusion.

[11] HIRAYAMA,T., SHIMIZU,K.,SHIRAI,H., et al.,15th European Conf. on Controlled Fusion and Plasma Heating, Dubrovnik, vol.3, (1988) 1065

[12] McCormick,K., SÖLDNER,F.X.,ECKHARTT,D., et al.
Phy. Rev. Lett. 58(1987)491.

[13] WHITE, R.B., MONTICELLO, D.A., ROSENBLUTH,M.N., et al.,
Phys. Fluids 20(1977)800.

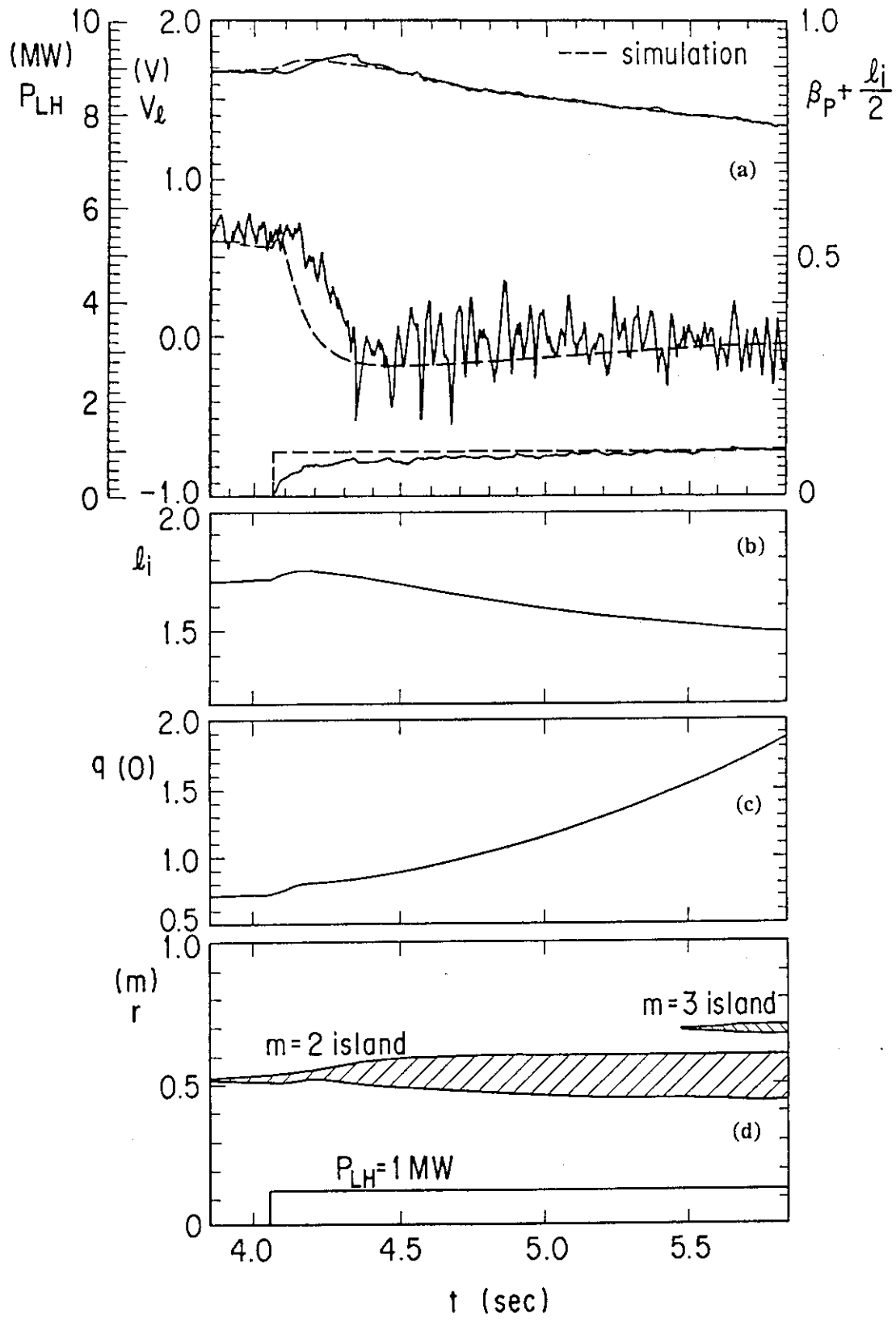

Fig.1 Time evolutions of LHCD.
(a)$\beta_p+l_i/2$, loop voltage, and injected power of LHRF. Solid lines: experimental data, Dotted lines: simulated results; (b)l_i, (c) q(0), and (d) the location and width of m/n=2/1 and 3/1 islands. All of (b),(c) and (d) are the results of a numerical simulation.

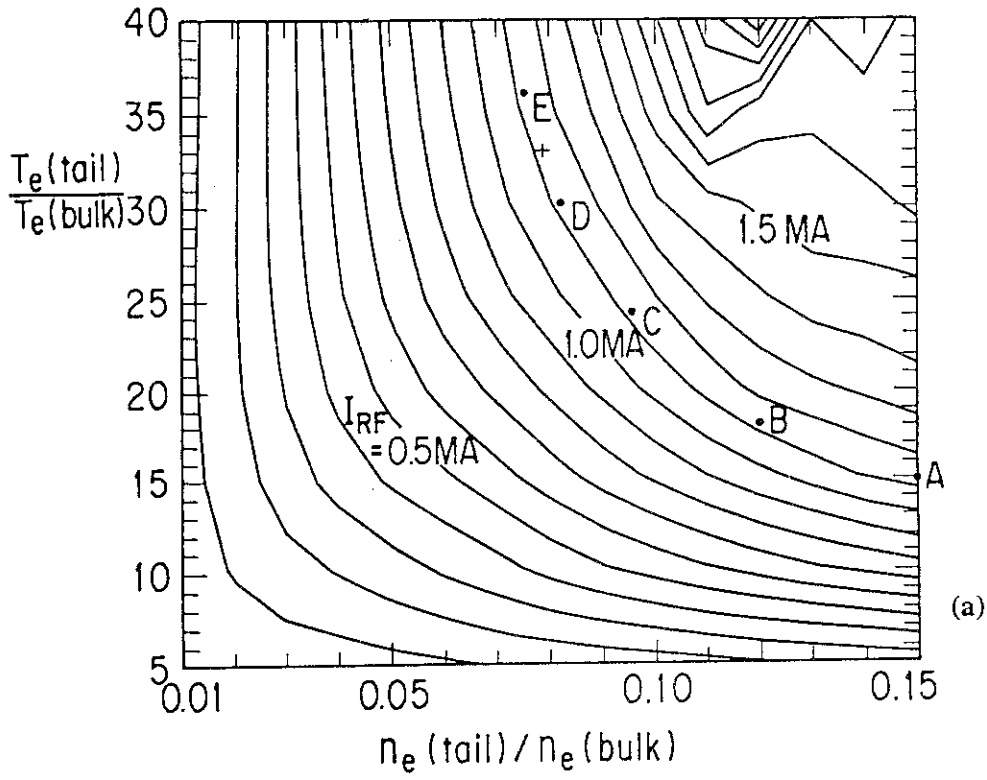

Fig.2.(a) Contours of the total RF current in the parameter plane of the high energy electron tail.
n_e(tail)/n_e(bulk) is the ratio of the tail electron density to the bulk electron density. Te(tail)/Te(bulk) is the temperature ratio of the tail to the bulk.

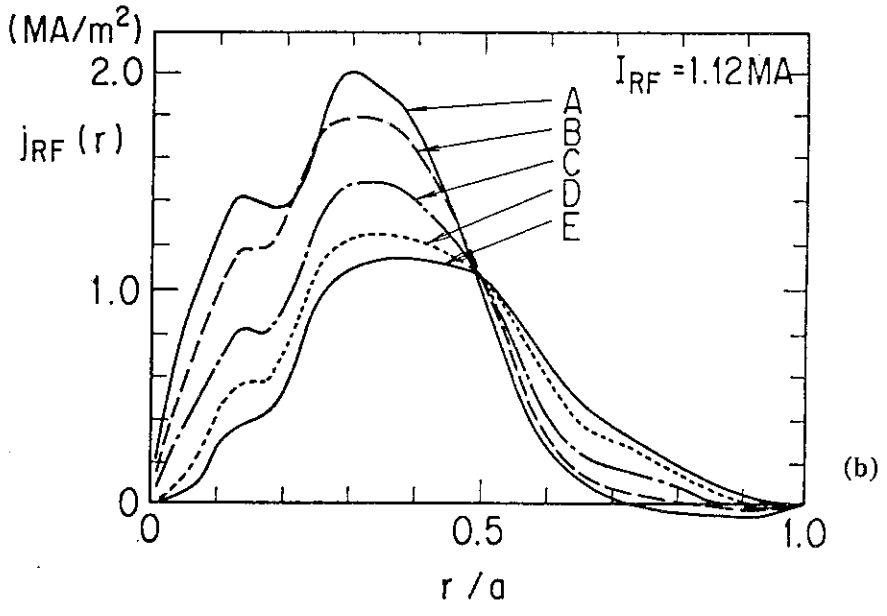

Fig.2(b) RF current profiles related to the tail parameter as denoted in A,B,C,D and E in Fig.2(a).

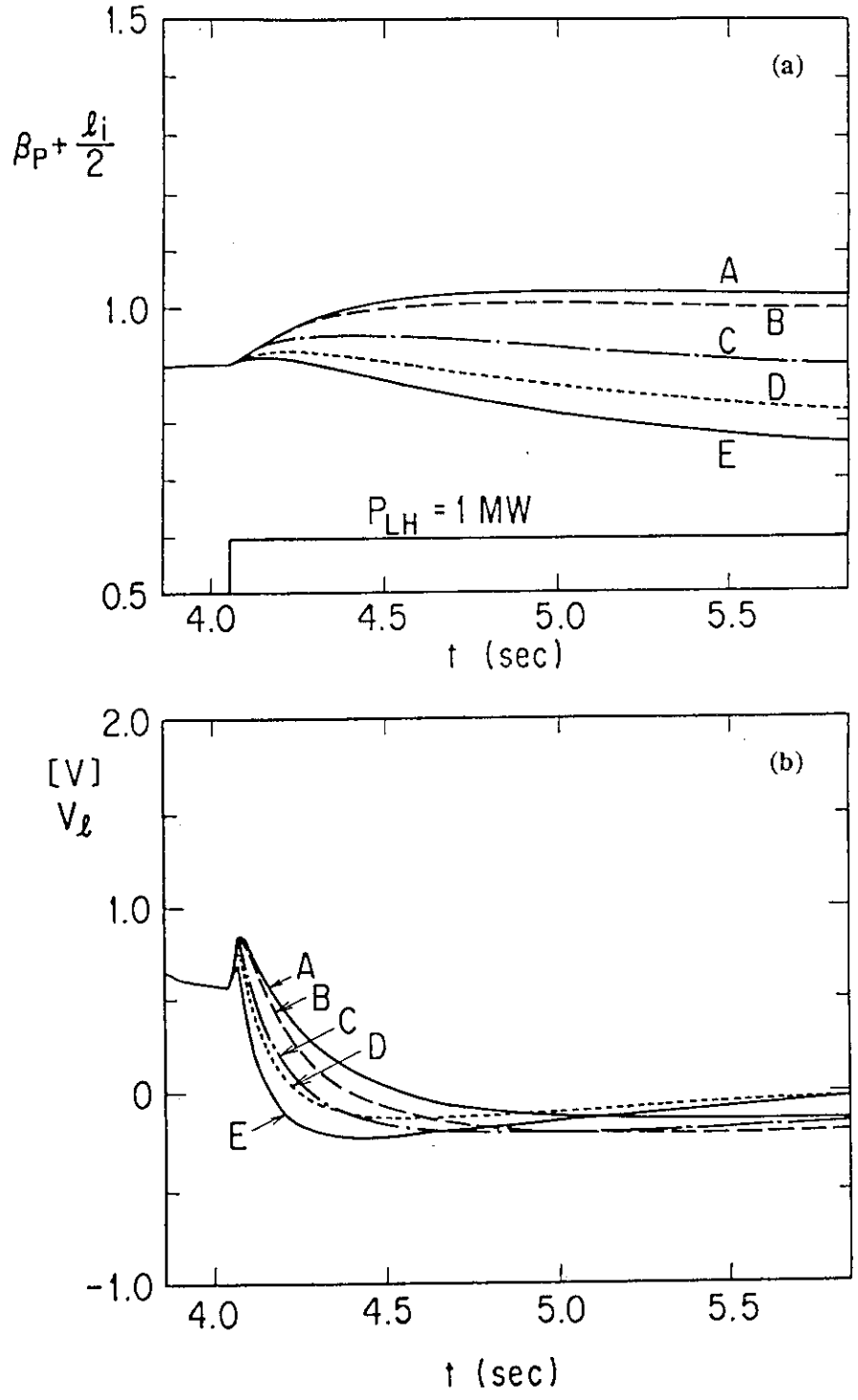

Fig.3 Time evolution of $\beta_p + l_i/2$ and loop voltage for the cases of A,B,C,D and E presented in Fig.2

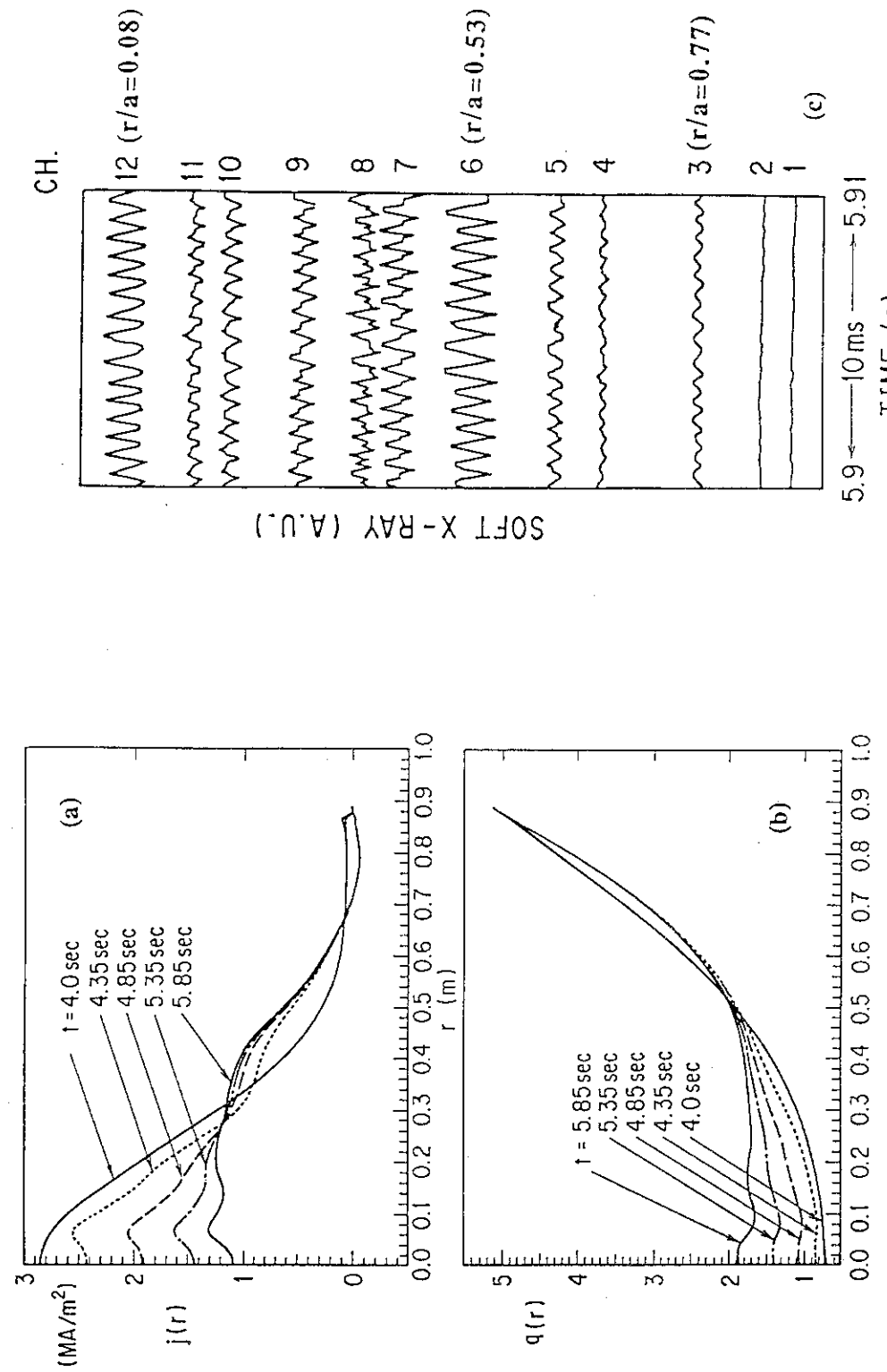

Fig.4 Time evolution of the profile of (a)current , and (b)safety factor, in the case of n_c(tail)/n_c(bulk)=0.078 and Te(tail)/Te(bulk)=33.0. (c)Fluctuation of each soft X-ray channcl signal at t=5.9sec.

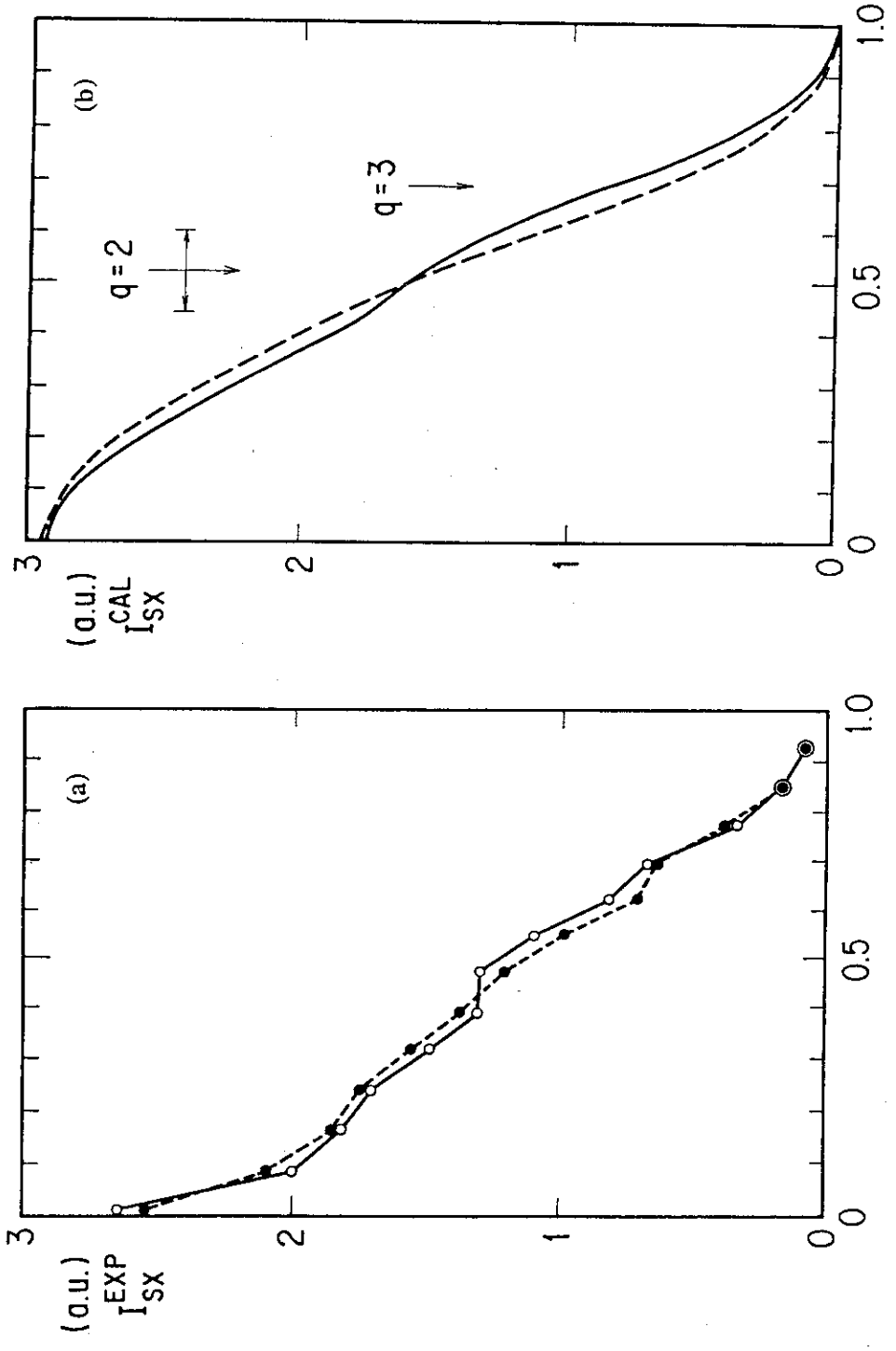

Fig.5 Soft X-ray emission profile.(a)Experimentally observed profile. (b)Calculated profile from the simulated m=2 island presented in Fig.1(d). The solid line; at the top in the fluctuation, the broken line; at the bottom in the fluctuation.